Published in final edited form as:
J Immunol. 2012 July 15; 189(2): 956–967. doi:10.4049/jimmunol.1102871.

Expression, Regulation and Function of Atypical Chemerin Receptor CCRL2 on Endothelial Cells

Justin Monnier[*,‡], **Susanna Lewén**[‡], **Edward O'Hara**[*], **Kexin Huang**[†], **Hua Tu**[†], **Eugene C Butcher**[*,‡], and **Brian A. Zabel**[‡]

[*]Laboratory of Immunology and Vascular Biology, Department of Pathology, Stanford University School of Medicine, Stanford, CA 94305, and Center for Molecular Biology and Medicine, Veterans Affairs Palo Alto Health Care System, Palo Alto, CA 94304

[†]LakePharma Inc, 530 Harbor Blvd Belmont, CA, 94002

[‡]Palo Alto Institute for Research and Education, Veterans Affairs Palo Alto Health Care System, 3801 Miranda Avenue, Palo Alto, CA 94304

Abstract

CC-chemokine receptor-like 2 (CCRL2) binds leukocyte chemoattractant chemerin and can regulate local levels of the attractant, but does not itself support cell migration. Here we show that CCRL2 and vascular cell adhesion molecule-1 (VCAM-1) are upregulated on cultured human and mouse vascular endothelial cells (EC) and cell lines by pro-inflammatory stimuli. CCRL2 induction is dependent on NF-κB and JAK/STAT signaling pathways, and activated endothelial cells specifically bind chemerin. *In vivo*, CCRL2 is constitutively expressed at high levels by lung endothelial cells and at lower levels by liver endothelium; and liver but not lung EC respond to systemic LPS injection by further upregulation of the receptor. Plasma levels of total chemerin are elevated in CCRL2−/− mice, and are significantly enhanced after systemic LPS treatment in CCRL2−/− mice compared to WT. Following acute LPS-induced pulmonary inflammation *in vivo*, CMKLR1+ NK cell recruitment to the airways is significantly impaired in CCRL2−/− mice compared to WT. *In vitro*, chemerin binding to CCRL2 on endothelial cells triggers robust adhesion of chemokine-like receptor-1 (CMKLR1)-positive lymphoid cells through an α4β1/VCAM-1-dependent mechanism. In conclusion CCRL2 is expressed by endothelial cells in a tissue and activation-dependent fashion; regulates circulating chemerin levels and its bioactivity; and enhances chemerin and CMKLR1-dependent lymphocyte-endothelial cell adhesion *in vitro* and recruitment to inflamed airways *in vivo*. Its expression and/or induction on EC by proinflammatory stimuli provide a novel and specific mechanism for the local enrichment of chemerin at inflammatory sites, regulating the recruitment of CMKLR1+ cells.

INTRODUCTION

Chemerin is a recently described chemotactic protein for dendritic cell subsets, macrophages, and natural killer cells (NK cells) (1–3). Chemerin circulates in an inactive pro-form: activation of chemerin requires proteolytic processing of the carboxyl-terminus and removal of inhibitory amino acids (4–7). We and others identified chemerin as a natural non-chemokine chemoattractant ligand for chemokine like receptor-1 (CMKLR1), and in a recent publication, we 'de-orphaned' an additional second receptor for chemerin, serpentine receptor CC-chemokine receptor-like 2 (CCRL2) (3, 5, 8–10). Interestingly, although both CCRL2 and CMKLR1 bind chemerin with high affinity, the downstream functional

Corresponding Author: Brian A. Zabel, bazabel@alum.mit.edu, (ph) 650-493-5000 x63132, (fax) 650-858-398.

consequences of ligand binding are quite different. Chemerin binding to CMKLR1 triggers calcium mobilization, receptor and ligand internalization, and cell migration. On the other hand, chemerin binding to CCRL2 does not induce intracellular calcium flux or ligand internalization, but can regulate chemerin bioavailability (3, 10). A third high affinity chemerin receptor, G-protein coupled receptor 1 (GPR1), has also been recently reported, although it also does not itself support chemerin-dependent cell migration (8).

Chemoattractants recruit leukocytes to inflamed tissues in part by triggering integrin-dependent adhesion to activated vascular endothelium. Several teams reported the co-localization of chemerin with vascular endothelial cells (EC) in multiple inflammatory disorders, such as multiple sclerosis, lupus, and psoriasis, and in endothelial venules of secondary lymphoid tissues (11–14). While several human endothelial cell lines express CMKLR1 and can respond to chemerin in an angiogenesis assay, CCRL2 has not yet been fully investigated in endothelial cell biology (15). Given the reported association of chemerin with vascular endothelial cells and the potential role of non-classical chemoattractant receptor CCRL2 in augmenting local chemerin levels we characterized the expression, regulation, and function of CCRL2 on human and murine vascular endothelial cells (10).

Here we report that pro-inflammatory stimuli upregulate atypical chemerin receptor CCRL2 and VCAM-1 on endothelial cells via NF-κB and JAK/STAT intracellular signaling pathways. Plasma chemerin levels are significantly elevated in CCRL2−/− mice following systemic LPS injection compared to WT mice and untreated controls, implicating CCRL2 in the regulation of circulating chemerin during inflammation. In an *in vivo* pulmonary inflammation model, recruitment of CMKLR1+ NK cells into the airways is impaired in CCRL2−/− mice. I*n vitro,* chemerin binding to CCRL2 positive endothelial cells triggers robust adhesion of CMKLR1+ lymphoid cells via α4β1/VCAM-1- mediated sticking. Thus CCRL2 on EC acts in concert with CMKLR1 to coordinate chemerin-dependent leukocyte adhesion *in vitro* and recruitment *in vivo*.

MATERIAL AND METHODS

Animals

CCRL2−/− mice were obtained from Lexicon (The Woodlands, TX, USA) and backcrossed 9 generations on the Balb/c background. WT Balb/c mice were obtained from Jackson Laboratories (Sacramento, CA, USA).

Reagents

Soluble Mediators—IL-1, IL-2, IL-4, IL-6, IL-10, IL-12, IL-13, IL-17, IL-23, CXCL12, GM-CSF, VEGF, Netrin4, FLT3L, TGFβ, IFNγ, TNFα, and chemerin were purchased from R&D systems (Minneapolis, MN, USA). LTA (TLR2), Flagellin (TLR5), R837 (TLR7), CpGa (TLR9), LPS (TLR4), Poly(I:C) (TLR3) were purchased from InvivoGen (San Diego, CA, USA). Vitamin D3, Vitamin D2, dexamethasone were obtained from Sigma (Saint Louis, MO, USA). IFNα, IFNβ were obtained from PBL Interferon Source (Piscataway, NJ, USA).

Primary Antibodies—Anti-mouse antibodies:α-mCCRL2 (clone BZ2E3, generated in-house), rat IgG2a isotype control (clone 9B5, generated in-house). α-mCMKLR1 (clone BZ194, generated in-house, rat IgG2a; clone BZ186, generated in-house, mIgG1), α-mGPR1 (clone BZ48, generated in-house, rat IgG2a), α-mVCAM (clone MK2.7, generated in-house, rat IgG1). Anti-mCD31-PEcy7, α-mCD146-FITC, α-mVCAM-1 APC (clone 429) were purchased from Biolegend (San Diego, CA, USA), anti-CD3-PECy7, anti-Ly6G-FITC,

and anti- DX5-PE were purchased from eBioscience (San Diego, CA, USA). Anti-human antibodies: α-hCMKLR1 (clone BZ332, generated in-house), α-hGPR1 (clone BZ1274, generated in-house, rat IgG2b);α-hVCAM-1-FITC (clone IE10), mouse IgG2b-FITC isotype control, and mouse-anti-human CCRL2 (clone 152211) were purchased from R&D Systems (Minneapolis, MN, USA).

Secondary Antibodies—Goat anti-rat IgG-PE (R&D Systems, Minneapolis, MN, USA), goat anti-human IgG-PE, rat anti-mouse-IgG PE (Invitrogen, Carlsbad, CA, USA), goat anti-mouse IgG Alexa-488 (Molecular Probes, Carlsbad, CA, USA).

Primers—mVCAM-1, hVCAM-1, hCMKLR1 were purchased from SA Bioscience (Valencia, CA, USA). Mouse-GPR1 (F-GGAGCTCAGCATTCATCACA, R-GACAGGCTCTTGGTTTCAGC), hGPR1 (F-AATGCCATCGTCATTTGGTT, R-CAACTGGGCAGTGAAGGAAT), hCCRL2 (F-GAGGCAGAGCAATGTGACAA, R-ATTTTTCCACGCGTTTGAGTC). Mouse-CCRL2, mCMKLR1, mChemerin, hChemerin and hβactin were used as previously described (10, 16, 17).

Inhibitors—IKKβ phopshorylation inhibitor BAY-11-7082 (Calbiochem, Gibbstown, NJ, USA), JAK-1 inhibitor sc-204021 (Santa Cruz-Biotech, Santa Cruz, CA, USA).

Primary Endothelial Cell Isolation

Mouse liver and lung endothelial cells were isolated from BALB/c wild-type and CCRL2−/− mice. Briefly, livers and lungs were isolated from 8–10 week old mice and digested in 5mg/ml PBS/Collagenase IV (Worthington, Lakewood, NJ, USA) for 45 min at 37C. Digested tissue was passed over cell strainers of decreasing size (100μM, 70μM, and 40μM) then centrifuged for 10 min at 300g at 4C. Endothelial cells were enriched using 30% Histodenz/RPMI solution (Sigma, Saint Louis, MO, USA), after centrifugation at 1500g for 20min at 4C, cells at the interface were collected and stained with CD31 (Biolegend, San Diego, CA, USA) and CD146 (Biolegend, San Diego, CA, USA) to identify the purified endothelial cell population.

Cell Culture

Mouse endothelial cell line culture—bEND.3 cells were grown in DMEM media (Gibco, Carlsbad, CA, USA), supplemented with pyruvate, non-essential amino acids, L-glutamine, penicylin-streptomycin and 10% FBS. For inhibitor experiments, bEND.3 cells were pre-incubated with the indicated concentration of inhibitor for 1 hour, after which fresh media +/− inhibitor with the indicated cytokines was added to the cells and incubated for an additional 24 hours. HEK-293 and L1.2 cells (pre-B cell mouse lymphoma) were grown in RPMI 1640 supplemented with pyruvate, non-essential amino acids, L-glutamine, penicylin-streptomycin, and 10% FBS and G418 (Gibco, Carlsbad, CA, USA).

Human Endothelial Cell Culture—HUVEC (human umbilical vein endothelial cells) and HDMEC (human dermal microvascular endothelial cells were purchased from (Lonza, Bazel, Switzerland) and a novel human brain microvascular endothelial cell line, hCMEC/D3, was obtained thanks to the generous gift of Prof. Courraut at the INSERM U1016 / CNRS UMR 8104 / Universite Paris Descartes (18). Briefly, cells were seeded at a concentration of 10.000 cells/ml on 0.02% gelatin coated plates. EBM media (Lonza) was changed every other day, and after 7 d confluent cells were ready for experimentation. 24 h prior to stimulation, cells were cultured in EBM base media containing reduced concentrations of supplemental growth factors.

RNA Isolation and RT-QPCR

Total RNA was extracted from cells using the RNeasy kit (Qiagen, Valencia, CA, USA), after which the total RNA concentration was measured using the Nanodrop spectrophotometer ND-100. RT-QPCR was performed using RT-Taq/SYBR green QPCR reagents (Invitrogen, Carlsbad, CA, USA) using a Stratagene Mx3000p thermocycler (Agilent, Santa Clara, CA, USA). Primers were validated using stringent criteria, by verifying that the dissociation curve showed only one peak, and "no Reverse Transcriptase" controls were used to confirm that QPCR results reflected RNA expression and not genomic DNA contamination. Gene expression was normalized to CDC42 for mouse samples and β-Actin for human samples. The relative induction value of our genes of interest was calculated using the $2^{-\Delta CT}$ method (19). All PCR reactions were done in duplicate.

Flow Cytometry

A total of 0.5 million cells were used for each staining. For unconjugated antibodies, cells were incubated with the indicated primary antibodies at 4°C for 30 min in 100 μl of PBS/ FBS 2% (Fetal Bovine Serum)/2% mouse serum. Cells were then washed with PBS and centrifuged for 3 min at 2000 rpm. Following the washing step, cells were incubated with secondary goat-anti rat PE (R&D systems, Minneapolis, MN, USA) in 50 μl of PBS/2% FBS/2% goat serum. For directly conjugated antibodies: cells are incubated with labeled antibody at 4°C for 30 min in 100 μl in PBS/2% FBS/2% mouse serum. Cells were washed and centrifuged for 3 min at 2000 rpm, resuspended and fixed in 200 μl of PBS/ 1%PFA (paraformaldehyde) and were analyzed using a FACS-Calibur (BD Biosciences, Franklin Lake, NJ, USA).

^{125}I-chemerin Binding Assay

For radioligand binding assays, radioiodinated chemerin (residues 21 – 148; R & D Systems; custom radiolabeling performed by PerkinElmer) was provided as a gift from J. Jaen (ChemoCentryx, Mountain View, CA). To assess the ability of chemerin to bind to bEND.3 cells treated with cytokines, 5×10^4 cells/per well were mixed with 4-fold dilutions of unlabeled chemerin competitor and ~ 1 nM (0.025 μCi) of ^{125}I-chemerin tracer per well in a total volume of 200 μl, and agitated at 4°C for 3 hours. Levels of cell-bound radioactivity were determined by harvesting the cells on poly (ethyleneimine)-treated GF/B glass filters (Perkin Elmer, Waltham, MA) using a cell harvester (Perkin Elmer), washing the filters twice with buffer (25 mM HEPES, 500 mM NaCl, 1 mM $CaCl_2$ and 5 mM $MgCl_2$, adjusted to pH 7.1) and measuring the amount of ^{125}I-chemerin bound to each filter (CPM) with a TopCount scintillation counter (Perkin Elmer, Waltham, MA, USA).

Fc-Chemerin

Recombinant Fc-Chemerin protein (residues 23–156) were produced and purified from CHO cells via transient transfection and Protein A purification. A DNA fragment corresponding to bioactive mouse chemerin isoform ending in residue 156 (serine) was amplified by PCR and cloned in-frame downstream of human or mouse IgG1 Fc domain, which is downstream of a secretion signal peptide in mammalian expression vector pLEV113 (LakePharma, Belmont, CA, USA). There is a 9 amino acid glycine-rich linker between the Fc and chemerin domain. Plasmid DNA was transfected into CHO cells using Lafectine transfection reagent (LakePharma, Belmont, CA, USA), and cell culture supernatant was collected 3–5 days post transfection. Fc fusion proteins were purified with Protein A resins (Mab Select SuRe GE Healthcare), and final proteins were formulated in 100 mM Tris (pH 7.5), 150 mM NaCl and 0.45% NaOAc.

Endothelial Cell Adhesion Assay

To assess the ability of CCRL2 on bEND.3 cells to induce adhesion, bEND.3 cells were grown to confluence in 96 well petri dishes. After 24h treatment with TNFα-LPS-IFNγ(20ng/ml, 1μg/ml and 50ng/ml respectively), bEND.3 cells were loaded with 50 μl of 200nM chemerin in PBS/BSA 0.1% and incubated at 37°C for 30 min. This step serves to load CCRL2 with chemerin. The cells are then washed with PBS to remove unbound chemerin. A 100μl of L1.2-CMKLR1 + cells at a concentration of 5×10^6 cells/ml, pre-labeled with calcein AM (BD Biosciences, Franklin Lake, NJ, USA), were placed on top of the bEND3 cells and let to co-incubate for 30 min at 37°C. The cells were washed 2 times with PBS without calcium and magnesium. The number of cells that adhered to the monolayer was then measured by a plate reader at an emission/excitation of 494/517. Pictures of adherent cells were taken using a fluorescent microscope. Blocking antibodies against VCAM-1 (MK2/7) and α4β1 (PS/2) were used at a concentration of 10μg/ml.

ELISA

Mice were injected intraperitoneally with LPS (12mg/kg), euthanized 12h later, and blood was collected by cardiac puncture. Plasma chemerin concentrations were measured by ELISA (R&D systems).

Chemerin Internalization Assay

HEK-293 cells transfected with hCMKLR1 or hCCRL2, bEND.3 cells, and HUVECs were used for chemerin internalization assays. One hundred thousand cells/well were incubated with mFc-hchemerin for 30min at 4°C and then washed with cold PBS to remove unbound chemerin. For the microscopy studies, HEK-293 transfectants and bEND.3 cells were incubated with secondary antibody goat-anti-mouse IgG Alexa 488 (molecular probes, Carlsbad, CA, USA). After 20 min incubation at 4°C the cells were washed in cold PBS. Subsequently, cells were either placed back at 4°C or incubated at 37°C to allow for labeled Fc-Chemerin to internalize. After a final wash in cold PBS, cells were fixed in PBS/1%PFA, and spun down on microscope slides by cytospin. Fc-Chemerin internalization was analyzed by epifluorescence microscopy. For the flow cytometry studies, Fc-Chemerin-loaded HUVECs were incubated at 4°C or 37°C for 30 minutes, washed, and then stained with secondary antibody goat-anti-mouse PE. Fc-Chemerin internalization was analyzed by flow cytometry.

Acute LPS-induced Lung Inflammation

WT and CCRL2 -KO mice were anesthetized and dosed with 1μg LPS in 50μl saline by intranasal injection. Twelve hours post-LPS injection the mice were euthanized and the leukocytes that accumulated in the airways were collected by broncheoalveolar lavage.

BAL Fluid Leukocyte Isolation

After mice were euthanized, a blunt needle was inserted in the exposed trachea. The airway of the mice was washed three times with 1 ml PBS. The recovered fluid was centrifuged and the recovered leukocytes in the BAL fluid were directly stained with surface markers for T cells (CD3), neutrophils (Ly6G), and NK cells (DX5).

Blood Leukocyte Isolation

Blood was collected by cardiac puncture after euthanasia and directly mixed with 5ml PBS without Ca2+/Mg2+ supplemented with 4 mM EDTA to prevent clotting. An equal volume of dextran-T-500 was added, the solution gently mixted by inversion, and incubated at 37°C for 45 min. The supernatant was collected and centrifuged and incubated with 2 ml red

blood cell lysis buffer (Sigma, St. Louis, MO, USA). The pelleted white blood cells were then stained and analyzed by flow cytometry.

In Vitro Transwell Chemotaxis

mCMKLR1/L1.2 cells were used to assess chemerin bioactivity by *in vitro* transwell migration as previously described (3). For migration experiments, 2.5×10^5 mCMKLR1/L1.2 cells in 100 μl chemotaxis media (either RPMI + 10% FCS for pro-chemerin activation experiments, or RPMI + 0.5% BSA for detection of bioactive chemerin in the absence of proteases) were added to the top wells of 5- μm pore transwell inserts (Corning Costar, Lowell, MA, USA), and 25 μl plasma samples in 600 μl media were added to the bottom wells. After incubating the transwell plates for 2 hours h at 37°C, the bottom well cells were harvested and flow cytometry was used to assess migration. To test the amount of pro-chemerin in the plasma samples, 25μl of plasma were incubated with 5 ul plasmin (1 mg/ml, reconstituted in PBS) for 5 minutes at 37°C, and then immediately diluted in 600 μl cold chemotaxis media (RPMI + 10% FBS).

Statistics

Evaluation of significance was performed using Student's *t*-test, or ANOVA followed by Bonferonni post-test. Statistical tests were calculated using the Instat statistical program (Graphpad, La Jolla, CA, USA), and graphs were plotted using Prism graphing software (Graphpad, La Jolla, CA, USA). Data is expressed as mean ± SD or SEM as indicated, and p-value less than 0.05 was considered to be significant.

RESULTS

CCRL2 and VCAM-1 are upregulated on mouse brain vascular endothelioma cells by pro-inflammatory cytokines and certain TLR ligands

Given the reported co-localization of chemerin with activated endothelial cells in multiple inflammatory diseases, we tested a panel of cytokines and TLR-ligands for CCRL2 induction in bEND.3 endothelioma cells, a model cell line of mouse brain vascular endothelial cells (11–14,20). A subset of pro-inflammatory cytokines and TLR-ligands (TNFα, LPS, IFNγ, IL-1β, IFNβ, and Poly(I:C) induced CCRL2 protein expression (Fig. 1A, 1B). The cytokines and factors that upregulated CCRL2 were similar to those that induced VCAM-1, although optimal upregulation of CCRL2 required synergistic activity of TNFα with other stimuli (e.g. IFNγ and LPS), whereas VCAM-1 was highly induced by TNFα alone (Fig. 1C, 1D), the latter observation is consistent with previous reports (20). Chemerin receptors CMKLR1 and GPR1 were not expressed under any condition, whether assessed by antibody staining or RNA analysis (data not shown).

Kinetics of CCRL2 and VCAM-1 RNA and protein induction in LPS, IFNγ, and TNFα treated bEND.3 cells

Consistent with the protein expression analysis, CCRL2 and VCAM-1 RNA were upregulated by pro-inflammatory stimuli (Fig. 2A, 2B). We next examined the RNA and protein induction kinetics of CCRL2 and VCAM-1 following treatment with TNFα, LPS, and IFNγ (Fig. 2B, D). RNA expression for both CCRL2 and VCAM-1 occurred rapidly and peaked after just two hours for each. Despite similar RNA induction kinetics, CCRL2 protein expression peaked at 24h post-treatment, whereas VCAM-1 surface expression peaked at 8h (Fig. 2C, 2D).

CCRL2 induction is controlled by NF-κB and JAK-STAT signaling pathways

The robust and synergistic induction of CCRL2 by the combination of TNFα LPS and IFNγ in bEND.3 cells prompted us to investigate the intracellular pathways involved. Previously, it was shown that TNFα and LPS trigger the intracellular NF-κB pathway in endothelial cells, whereas IFNγ activates the JAK-1/STAT-1 pathway; however, more recent evidence indicates that TNFα and LPS can also activate the STAT-1 pathway, and, conversely, that IFNγ can indirectly stimulate the NF-κB pathway (21–23). To test the role of NF-κB and JAK-1/STAT-1 in the upregulation of CCRL2, we used pharmacoinhibitors of the NF-κB pathway (BAY 11-7082) and of the JAK-1/STAT-1 pathway (sc-204021). The NF-κB inhibitor almost completely prevented the induction of CCRL2 in bEND.3 cells by TNFα, LPS, and Poly (I:C), but only partially inhibited IFNγ– or IFNβ– dependent CCRL2 induction (Fig. 3). On the other hand, the JAK-1 inhibitor marginally inhibited TNFα, LPS, IL-1β, or Poly(I:C) induced induction of CCRL2, but almost completely blocked IFNγ– or IFNβ– dependent CCRL2 induction (Fig. 3). Cells treated with NF-κB or JAK inhibitors only partially blocked CCRL2 induction when TNFα, LPS and IFNγ were combined together. However, the combination of both NF-κB and JAK-1 inhibitors almost completely blocked CCRL2 induction by combined TNFα, LPS and IFNγ, suggesting that both pathways are involved and that they can independently and synergistically upregulate endothelial CCRL2 (Fig. 3).

Activated bEND.3 cells bind chemerin

Excess unlabeled chemerin inhibited the binding of either ^{125}I-chemerin (IC_{50}: 3 nM, Fig. 4A) or Fc-Chemerin (IC_{50}: 8 nM, Fig. 4B) to bEND.3 cells treated with pro-inflammatory stimuli. Chemerin did not bind to unstimulated bEND.3 cells (Fig. 4).

Expression and regulation of CCRL2 in human endothelial cells

Primary human umbilical vein and dermal microvascular endothelial cells (HUVECs and HDMECs, respectively), as well as a human brain endothelial cell line (hCMEC/D3) significantly upregulated CCRL2 RNA following exposure to TNFα, LPS, and IFNγ (Fig. 5A). VCAM-1 RNA was also significantly upregulated as anticipated (data not shown). Furthermore, unstimulated HUVECs expressed CCRL2 protein and bound Fc-Chemerin; and stimulation with TNFα, LPS, and IFNγ slightly increased CCRL2 protein expression and Fc-Chemerin binding (Fig. 5B).

Expression and regulation of CCRL2 on mouse primary endothelial cells

We next asked if CCRL2 was expressed on freshly isolated mouse vascular lung and liver endothelial cells, as these organs provided an adequate quantity of primary EC for analysis. Interestingly, CD31+CD146+ mouse lung endothelial cells expressed high levels of CCRL2 in the absence of experimental exogenous activation, and mouse liver endothelial cells were moderately positive. Antibodies against CCRL2 failed to stain lung or liver endothelial cells from CCRL2-deficient mice, confirming the specificity of the antibody staining. We did not detect any genotype-dependent differences inVCAM-1, CD31 or CD146 expression on lung or liver EC, suggesting that overall the endothelial cell phenotype is not altered in the CCRL2-deficient animal (Fig. 6A, B).

In vivo injection of LPS upregulates CCRL2 on liver endothelial cells

LPS injection activates vascular endothelial cells *in vivo*(24,25). To ask if endothelial CCRL2 is induced by LPS *in vivo*, we injected mice systemically with endotoxin, isolated vascular EC from liver and lung, and assessed CCRL2 and VCAM-1 expression and chemerin binding by flow cytometry. CD31+CD146+ liver endothelial cells from LPS-injected WT mice significantly upregulated CCRL2 and bound to Fc-Chemerin, while

similar cells from saline-injected WT mice were CCRL2^{low} (Fig. 7A). LPS injection had no effect on CCRL2 expression or Fc-Chemerin binding to WT lung endothelial cells relative to isotype control staining (Fig. 8). Furthermore, neither CCRL2 antibody nor Fc-Chemerin stained liver or lung endothelial cells from LPS-injected or control CCRL2−/− mice (Fig. 7, 8). Consistent with previous reports, LPS injection upregulated VCAM-1 on liver and lung endothelial cells in both genotypes (Fig. 7, 8) (24, 26–29).

Endothelial cell CCRL2 captures and concentrates chemerin on the cell surface

Given our previous data that CCRL2+ lymphoid cells do not internalize bound chemerin, we next asked if CCRL2+ vascular endothelial cells also concentrated chemerin on the cell surface. CCRL2+ bEND.3 cells (treated with TNFα, LPS, and IFNγ) bound to Fc-Chemerin, while untreated cells were negative for chemerin binding (Fig. 9A). Upon shifting the chemerin-loaded cells to an internalization-permissive temperature (37°C), the bEND.3 cells did not internalize bound ligand (Fig. 9A). CCRL2+ HEK-293 transfectants also did not internalize bound Fc-Chemerin, however, CMKLR1+ HEK-293 cells efficiently internalized bound Fc-Chemerin when incubated at 37°C, as evidenced by the cytoplasmic puncti and lack of membrane staining (Fig. 9B). To ask if these results extend to primary human endothelial cells, Fc-Chemerin-loaded HUVECs (stimulated with TNFα+LPS +IFNγ) were incubated at 4°C or 37°C, washed, and then stained for surface chemerin. The staining intensity of surface Fc-Chemerin on HUVECs incubated at 37°C was similar to the staining intensity at 4°C, indicating that HUVECs did not internalize bound chemerin (Fig. 9C).

CCRL2 regulates circulating chemerin levels *in vivo*

Given the constitutive expression of CCRL2 lung vascular EC and, to a lesser extent liver vascular EC, we hypothesized that circulating chemerin levels may be altered in CCRL2−/− mice due to lack of chemerin sequestration in the vasculature. Indeed, plasma levels of total chemerin (measured by ELISA, which detects bioactive chemerin, pro-chemerin, and larger fragments of chemotactically inert chemerin) were slightly but significantly elevated in CCRL2−/− mice compared to WT (Fig 10A). There was no significant difference in the level of bioactive plasma chemerin between WT and CCRL2−/− (Fig. 10B), and there was a slight but non-significant increase in pro-chemerin (detected by *ex vivo* proteolytic (plasmin) activation) in CCRL2−/− plasma compared with WT (Fig. 10C), as measured by *in vitro* CMKLR1 + cell migration. Interestingly, in mice dosed with endotoxin to induce systemic inflammation and vascular CCRL2 expression, total chemerin plasma levels were 2-fold higher in CCRL2−/− mice vs. WT, and 2-fold higher than untreated CCRL2−/− controls (Fig. 10A). While there was no difference in bioactive plasma chemerin levels between LPS-treated WT and CCRL2−/− (Fig. 10B), pro-chemerin levels in CCRL2−/− plasma were significantly elevated compared with WT (Fig. 10C). Taken together, these data indicates that the increase in total circulating chemerin in LPS-treated CCRL2−/− mice is due to an increase in pro-chemerin and possibly inactive chemerin fragments. Interestingly, plasma levels of bioactive chemerin and pro-chemerin were significantly reduced in LPS-treated WT compared with untreated controls (Fig. 10B, C). Although plasma from CCRL2−/− mice showed a similar trend, the differences did not reach significance (Fig. 10B, C). Thus, CCRL2 regulates circulating chemerin levels and its proteolytic processing *in vivo* during systemic inflammation.

To isolate the role of vascular endothelium-expressed CCRL2 in regulating circulating chemerin levels, mice were injected intravenously with Fc-Chemerin and the levels of plasma Fc-Chemerin (as opposed to total chemerin) were measured over time. Plasma Fc-Chemerin levels were significantly higher in CCRL2−/− mice compared with WT controls

(AUC_{CCRL2}−/−: 40,540 ± 2,630 ng h/ml vs. AUC_{WT}: 29,550 ± 1,240 ng h/ml, *p <0.05 by *t*-test, Fig. 10D).

Impaired CMKLR1+ NK cell trafficking into inflamed airways in CCRL2−/− mice

Intranasal injection of LPS causes acute lung inflammation and the accumulation of leukocytes into the broncheoalveolar space (30). Given the high level of CCRL2 expression and chemerin binding by lung EC, we used this pulmonary inflammation model to ask if CCRL2-deficiency altered the accumulation of CMKLR1 + NK cells into inflamed airways. Although there were no genotype-dependent differences in the total number of BAL infiltrating leukocytes, T cells or neutrophils, significantly fewer NK cells (measured as absolute number and as a percentage of total BAL leukocytes) accumulated in the airways of CCRL2−/− mice (Fig. 11A,B,C). Blood NK cells from WT and CCRL2−/− mice expressed similar levels of CMKLR1 (Fig. 11D) and Fc-Chemerin binding (not shown), ruling out differential CMKLR1 receptor expression as a contributing factor in impaired airway NK cell trafficking in CCRL2−/− mice. NK cells themselves are CCRL2-negative (data not shown). In addition, there were no differences in total numbers (or percent) of circulating NK cells (or other major leukocyte subsets, such as neutrophils) between CCRL2−/− and WT mice (Fig. 11E and data not shown). Thus, CCRL2 deficiency selectively impairs the recruitment of CMKLR1 + NK cells in an *in vivo* model of airway inflammation.

Chemerin bound to CCRL2+ endothelial cells triggers CMKLR1+ cell adhesion

CCRL2 binds chemerin such that the critical cell-signaling carboxyl-terminus remains exposed at the cell surface (10), and chemerin triggers CMKLR1 + macrophage adhesion by inducing α4β1 integrin clustering and binding to VCAM-1-coated plates (31). Since activated bEND.3 cells express high levels of both VCAM-1 and CCRL2 (Fig. 1), and L1.2 lymphoid cells express endogenous α4β1 (32), we hypothesized that CCRL2 on bEND.3 cells could bind chemerin and trigger CMKLR1 + L1.2 cell adhesion (33). Using a static endothelial adhesion assay, we compared the ability of WT or CMKLR1 + L1.2 cells to adhere to untreated or activated CCRL2+ bEND.3 cells in the presence or absence of chemerin. Activated CCRL2+ endothelial cells loaded with chemerin triggered significant and robust adhesion of CMKLR1+ L1.2 cells compared with un-stimulated CCRL2- endothelial cells (Fig. 12A, B). WT L1.2 cells did not adhere to the endothelial monolayer under any condition tested, and chemerin was required for adhesion-triggering (Fig. 12A). Blocking antibodies against α4 or VCAM-1 abolished chemerin-dependent CMKLR1+ cell adhesion to CCRL2+ activated endothelium, confirming that the adhesion molecules that mediate cell sticking in this model are α4β1 and VCAM-1 (Fig. 12C).

DISCUSSION

Chemerin is associated with vascular endothelium in the affected tissues of multiple inflammatory disorders, such as MS, lupus, and psoriasis (11–14), yet little is known regarding the regulation and role of its receptors on endothelial cells. Here we show that in a variety of endothelial cells, CCRL2, a high affinity chemerin receptor, is either constitutively expressed (lung EC, liver EC, and HUVEC) and/or induced (bEND.3, hCMEC/D3, HDMEC, HUVEC, and liver EC) by pro-inflammatory stimuli. As with lymphoid cell-expressed receptor, CCRL2 on EC binds chemerin but does not internalize the ligand. Chemerin bound to CCRL2+ endothelial cells triggered robust adhesion of CMKLR1+ lymphoid cells via α4β1/VCAM-1 interactions (illustrated in Fig. 12D). *In vivo*, CCRL2-deficiency resulted in selective impairment of CMKLR1+ NK cell accumulation into the airways following experimental pulmonary inflammation. Thus, our data suggests that CCRL2 on EC functions to increase local concentrations of chemerin and recruit CMKLR1+ cells to sites of inflammation.

Although we tested an array of pro-inflammatory and immune suppressive cytokines, interleukins, growth factors, and TLR ligands, only pro-inflammatory stimuli (TNFα, IFNγ, IFNβ, LPS, and Poly(I:C) induced CCRL2 on the mouse brain endothelial model cell line bEND3. In addition, pro-inflammatory factors induced CCRL2 in three human endothelial model cell lines (HUVEC, HDMEC, and hCMEC/d3). We and other reported similar results for CCRL2 induction by mouse peritoneal macrophages and dendritic cells [8, 27], suggesting the involvement of shared pathways for CCRL2 regulation across cell types. Endothelial cells express TNFαR, IFNγR, IFNβR, TLR4, and TLR3, consistent with responsiveness (as measured by CCRL2 or VCAM-1 induction) to their respective ligands (34–37). Combinations of pro-inflammatory mediators were significantly more robust in triggering CCRL2 induction than any individual stimuli (maximal response with TNFα/LPS/IFNγ), consistent with enhanced induction of CCRL2 on human neutrophils by co-treatment with TNFα and IFNγ (38), implying that multiple intracellular signaling pathways (NF-κB, JAK/STAT and possibly others) work synergistically to regulate CCRL2 expression. Indeed, treating cells with pharmacoinhibitors targeting both NF-κB and JAK/STAT pathways significantly reduced CCRL2 induction by TNFα/LPS/IFNγ. Furthermore, the addition of immune suppressive factors such as dexamethasone, TGFβ or IL-10 failed to inhibit the TNFα/LPS-stimulated induction of CCRL2 or VCAM-1, indicating that the pro-inflammatory signals are dominant (Fig. 1).

To confirm that the endothelioma cell lines accurately reflected primary EC biology, we evaluated CCRL2 expression on freshly isolated lung and liver endothelial cells from mice dosed with endotoxin to induce systemic inflammation and vasculitis (24). Systemic administration of endotoxin has been reported to increase circulating levels of TNFα and IFNγ, mimicking to an extent the *in vitro* stimulation of CCRL2 on endothelial cells (24, 25). Indeed, liver endothelial cells upregulated CCRL2 in response to LPS challenge *in vivo*. Interestingly, endothelial cells isolated from the lung of normal WT mice constitutively expressed CCRL2 and bound Fc-Chemerin, but LPS treatment did not alter lung CCRL2 expression. Primary human endothelial cells (HUVEC and HDMEC) treated *in vitro* with pro-inflammatory stimuli upregulated CCRL2 and bound Fc-Chemerin, indicating conserved regulation in primary EC across species. Liver and lung endothelial cells from LPS-dosed mice of both genotypes upregulated VCAM- 1, which is consistent with previous reports (24, 26, 39). It is not yet clear why CCRL2 is expressed endogenously at higher levels in mouse lung ECs compared to liver ECs, although it is well documented that ECs isolated from anatomically different vascular beds are phenotypically and functionally distinct in leukocyte adhesion and trafficking mechanisms (20, 40, 41).

Given prior reports indicating CMKLR1 expression and function in cultured EC *in vitro* (15, 42) we monitored CMKLR1 and GPR1 protein (and in most cases RNA) expression in bEND.3, hCMEC/D3, HUVEC, HDMEC, and primary mouse lung and liver EC. In all conditions tested, endothelial cells did not express CMKLR1 or GPR1at the protein or RNA level (data not shown). Part of the discrepancy may be due to different culture conditions, which could affect gene regulation (15). However, liver and lung EC from LPS-dosed CCRL2-deficient mice did not bind to Fc-Chemerin, thus indicating that CCRL2 is the primary receptor for chemerin on liver and lung ECs *in vivo*.

With its lack of classical signaling responses (i.e. cell migration, intracellular calcium mobilization) and absence of a ‘DRY’ motif in the second intracellular loop (thought to enable coupling to G-proteins (43)), CCRL2 may be considered a member of the family of atypical chemoattractant receptors that include DARC, D6, CCX-CKR, and CXCR7, (reviewed in (44)). These receptors modulate immune responses by regulating the bioavailability of chemoattractants, usually through specialized and efficient ligand internalization and degradation (44, 45). Mice deficient in D6 or DARC, for example, show

increased inflammation in models of skin inflammation and endotoxemia respectively, due to impaired chemokine clearance (46, 47). In line with their biological function to intercept excess circulating chemokines, D6, DARC and CXCR7 are widely expressed on numerous endothelial cell types (48–50). CCRL2 is also expressed on a variety of endothelial cells from different tissues (brain, skin, lung and liver), suggesting a role for CCRL2 in regulating the bio-availability of circulating chemerin. Indeed, the intravascular time-integrated chemerin levels over two weeks following a single i.v. injection of Fc-Chemerin was significantly greater (by 40%) in CCRL2−/− mice compared to WT. This is also likely reflected in the small but significantly elevated plasma chemerin levels in unchallenged CCRL2−/− mice. Furthermore, treatment of mice with endotoxin, which upregulates vascular EC CCRL2 and enhances chemerin binding in WT mice, produced a robust 2–3 fold greater than WT increase in circulating chemerin levels in CCRL2−/− mice. Other examples of increased chemoattractant levels in mice deficient for their cognate receptor include CCL2/CCR2 and chemerin/CMKLR1 in a model of pneumonia (51, 52). Although a contribution of extravascular CCRL2 is not formally excluded by our studies, CCRL2 control of circulating chemerin levels most likely occurs at the level of vascular EC. Thus, in regulating the bioavailability of leukocyte attractant chemerin, CCRL2 exhibits another trait in common with the other atypical chemoattractant “interceptors”. However, one critical difference that sets CCRL2 apart from the other atypical receptors is that CCRL2 does not internalize bound chemerin, demonstrated here with EC and previously with CCRL2+ lymphoid cells (10).

Chemerin circulates in an inactive pro-form, and requires proteolytic processing to increase its biological activity. It is tempting to speculate that CCRL2 could bind and present pro-chemerin on the surface of endothelial cells to circulating serine proteases widely present during endotoxaemia, thus removing the inhibitory peptides and presenting the active chemerin to circulating CMKRL1+ cells (reviewed in (53)). Other surface bound receptors such as endothelial protein C receptor (EPCR) are known to bind and concentrate their soluble ligand on the surface of ECs allowing for more efficient proteolytic activation by their cognate enzyme. Indeed, EPCR is widely expressed on vessels and binds and concentrates protein C, accelerating by 20-fold the activation of protein C by thrombin (54, 55). If EC CCRL2 captures circulating pro-chemerin and enhances its proteolytic activation during inflammation, we would predict 1) a reduction in circulating pro-chemerin levels in LPS-treated WT mice vs. untreated WT controls, and 2) an increase in circulating pro-chemerin in LPS-treated CCRL2−/− mice compared with WT. Indeed, there was significantly less circulating pro-chemerin in WT LPS-treated mice compare with untreated WT controls, likely reflecting sequestration by EC CCRL2 during systemic inflammation (Fig. 10B). In addition, there was significantly more plasma pro-chemerin in LPS-treated CCRL2−/− mice than WT mice (Fig. 10C), along with a significant 2–3 fold increase in total circulating chemerin levels (Fig. 10A). Thus, our results are consistent with the hypothesis that EC CCRL2 binds plasma pro-chemerin for enhanced proteolytic activation during inflammation. Additional work is necessary to characterize protease-specific effects of CCRL2-dependent anchoring of chemerin in its proteolytic activation.

Depending on the model, chemerin and its receptors CCRL2 and CMKLR1 can play a pathogenic or protective role in pulmonary inflammation: CMKLR1 plays a pathogenic role in cigarette-smoke induced lung inflammation (56) and CCRL2 plays a pathogenic role in an ovalbumin model of lung inflammation (57), whereas CMKLR1 plays a protective role in viral pneumonia and an LPS-airway challenge model (30, 51). Given the robust expression of CCRL2 on lung EC and the recent reported contributions of the chemerin receptors to leukocyte recruitment during pulmonary inflammation, we investigated the role of CCRL2 in CMKLR1+ NK cell recruitment to the airways in response to intranasal LPS challenge. We hypothesized that EC CCRL2-dependent anchoring/accumulation of bioactive chemerin

contributes to the recruitment of CMKLR1+ NK cells to inflamed airways, an effect that should be attenuated in CCRL2-deficient mice. Indeed, significantly fewer CMKLR1+ NK cells accumulated in the airways of CCRL2−/− mice compared to WT (Fig. 11). There were no differences in the recruitment of CMKLR1-negative neutrophils or CD3+ cells. In addition, there were similar numbers of circulating NK cells and other major white blood cell subsets in CCRL2−/− and WT mice; a similar expression of CMKLR1 on NK cells from both genotypes; and a lack of expression of CCRL2 on NK cells. Taken together, these results indicate that CCRL2 selectively coordinates the recruitment of CMKLR1+ NK cells in a manner consistent with our model of EC CCRL2-dependent chemerin anchoring.

When bound to CCRL2, the carboxyl-terminus of chemerin important for CMKLR1 signaling remains exposed at the cell surface (10). Recently, Hart et al. demonstrated that chemerin is a potent inducer of CMKLR1+ peritoneal macrophage adhesion to VCAM-1 by inducing α4β1 clustering (31). Thus, we hypothesized that CCRL2+ EC could bind and effectively present chemerin to CMKLR1+ lymphoid cells to trigger cell adhesion. Adhesion of L1.2 lymphoid cells to EC required the following components: 1) CCRL2+ activated EC, 2) CMKLR1+ L1.2 cells and 3) chemerin. Furthermore, adhesion of CMKLR1+ cells was completely dependent on α4β1 and VCAM-1. Thus, we propose the following possible mechanisms to describe the concerted actions of CCRL2, CMKLR1, and chemerin: 1) *Direct mechanism*: CCRL2 directly presents chemerin to CMKLR1+ cells and thus creates a trio with CCRL2 binding the N-terminus, while CMKLR1 interacts with the critical signaling C-terminus of chemerin. 2) *Indirect mechanism*: Chemerin binds to CCRL2 with an affinity typical for a chemoattactant:receptor pair (low nanomolar Kd) (10); coupled with the lack of ligand internalization, it is likely that chemerin is released from the cell surface at a certain rate dependent on receptor density, temperature, pH, salt concentration, etc. and at some rate reacquired by CCRL2. Elevated local concentrations of soluble chemerin in the media near the CCRL2 cells, however, may trigger CMKLR1 activation and, subsequently, integrin α4β1 avidity upregulation, without requiring a trio complex.

In conclusion, our results provide a novel mechanism by which the chemoattractant chemerin is presented by CCRL2+ EC to trigger CMKLR1+ cell adhesion. Extracellular matrix glycosaminogylcans (GAGs) on the luminal side of the endothelium and are thought to immobilize and present chemokines to rolling leukocytes, which triggers integrin activation and leukocyte extravasation (58). In several human inflammatory disorders (MS, lupus, and psoriasis) in which chemerin is associated with inflamed endothelium, CMKLR1+ leukocytes (NK cells, plasmacytoid DCs) are found to infiltrate into the affected tissues (11–14). Furthermore, in two separate *in vivo* inflammatory models, CCRL2−/− mice displayed less severe allergic inflammation (10) and less severe ovalbumin-induced airway inflammation than WT counterparts (57); however, it is not clear if this protective effect is linked with a decrease in CMKLR1+ cell recruitment. Although GAGs likely play a role in chemerin binding (chemerin binds to heparin, a type of GAG), we hypothesize that CCRL2 expressed on inflamed endothelium provides a novel specific and selective mechanism to bind and concentrate chemerin (3). A recent report indicates that CCL19 may be an alternate chemoattractant ligand for CCRL2, thus widening the biological spectrum of action for CCRL2 (59). Nevertheless, selective inhibition of CCRL2 binding to chemerin, rather than inhibition of GAGs, which bind all chemokines, could be a novel targeted therapeutic strategy to block chemerin mediated recruitment of CMKLR1+ leukocytes in chemerin-associated inflammatory diseases, such as EAE/MS (13, 16).

Acknowledgments

This work was supported by NIH grant AI-079320 to BAZ; by grants R01 AI093981 and R37 AI047822 from the NIH and a Merit Award from the Department of Veterans Affairs to ECB; by fellowships from NIH T-32 training grant T32-AI07290-25, T32-AI07290-24 and American Cancer Society post-doctoral fellowship PF-12-052-01-CSM to JM; and by the FACS Core Facility of the Stanford Digestive Disease Center under P30 DK056339.

We thank Prof. Courraut at the INSERM U1016 / CNRS UMR 8104 / Universite Paris Descartes for providing us with the human brain endothelioma cell line hCMEC/d3. We thank Thomas Burke for technical assistance.

References

1. Skrzeczynska-Moncznik J, Stefanska A, Zabel BA, Kapinska-Mrowiecka M, Butcher EC, Cichy J. Chemerin and the recruitment of NK cells to diseased skin. Acta Biochim Pol. 2009; 56:355–360. [PubMed: 19543554]
2. Zabel BA, Ohyama T, Zuniga L, Kim JY, Johnston B, Allen SJ, Guido DG, Handel TM, Butcher EC. Chemokine-like receptor 1 expression by macrophages in vivo: regulation by TGF-beta and TLR ligands. Exp Hematol. 2006; 34:1106–1114. [PubMed: 16863918]
3. Zabel BA, Silverio AM, Butcher EC. Chemokine-like receptor 1 expression and chemerin-directed chemotaxis distinguish plasmacytoid from myeloid dendritic cells in human blood. J Immunol. 2005; 174:244–251. [PubMed: 15611246]
4. Busmann A, Walden M, Wendland M, Kutzleb C, Forssmann WG, John H. A three-step purification strategy for isolation of hamster TIG2 from CHO cells: characterization of two processed endogenous forms. J Chromatogr B Analyt Technol Biomed Life Sci. 2004; 811:217–223.
5. Wittamer V, Bondue B, Guillabert A, Vassart G, Parmentier M, Communi D. Neutrophil-mediated maturation of chemerin: a link between innate and adaptive immunity. J Immunol. 2005; 175:487–493. [PubMed: 15972683]
6. Wittamer V, Franssen JD, Vulcano M, Mirjolet JF, Le Poul E, Migeotte I, Brezillon S, Tyldesley R, Blanpain C, Detheux M, Mantovani A, Sozzani S, Vassart G, Parmentier M, Communi D. Specific recruitment of antigen-presenting cells by chemerin, a novel processed ligand from human inflammatory fluids. J Exp Med. 2003; 198:977–985. [PubMed: 14530373]
7. Zabel BA, Allen SJ, Kulig P, Allen JA, Cichy J, Handel TM, Butcher EC. Chemerin activation by serine proteases of the coagulation, fibrinolytic, and inflammatory cascades. J Biol Chem. 2005; 280:34661–34666. [PubMed: 16096270]
8. Barnea G, Strapps W, Herrada G, Berman Y, Ong J, Kloss B, Axel R, Lee KJ. The genetic design of signaling cascades to record receptor activation. Proc Natl Acad Sci U S A. 2008; 105:64–69. [PubMed: 18165312]
9. Meder W, Wendland M, Busmann A, Kutzleb C, Spodsberg N, John H, Richter R, Schleuder D, Meyer M, Forssmann WG. Characterization of human circulating TIG2 as a ligand for the orphan receptor ChemR23. FEBS Lett. 2003; 555:495–499. [PubMed: 14675762]
10. Zabel BA, Nakae S, Zuniga L, Kim JY, Ohyama T, Alt C, Pan J, Suto H, Soler D, Allen SJ, Handel TM, Song CH, Galli SJ, Butcher EC. Mast cell-expressed orphan receptor CCRL2 binds chemerin and is required for optimal induction of IgE-mediated passive cutaneous anaphylaxis. J Exp Med. 2008; 205:2207–2220. [PubMed: 18794339]
11. Vermi W, Lonardi S, Morassi M, Rossini C, Tardanico R, Venturini M, Sala R, Tincani A, Poliani PL, Calzavara-Pinton PG, Cerroni L, Santoro A, Facchetti F. Cutaneous distribution of plasmacytoid dendritic cells in lupus erythematosus. Selective tropism at the site of epithelial apoptotic damage. Immunobiology. 2009; 214:877–886. [PubMed: 19625100]
12. Albanesi C, Scarponi C, Pallotta S, Daniele R, Bosisio D, Madonna S, Fortugno P, Gonzalvo-Feo S, Franssen JD, Parmentier M, De Pita O, Girolomoni G, Sozzani S. Chemerin expression marks early psoriatic skin lesions and correlates with plasmacytoid dendritic cell recruitment. J Exp Med. 2009; 206:249–258. [PubMed: 19114666]
13. Lande R, Gafa V, Serafini B, Giacomini E, Visconti A, Remoli ME, Severa M, Parmentier M, Ristori G, Salvetti M, Aloisi F, Coccia EM. Plasmacytoid dendritic cells in multiple sclerosis: intracerebral recruitment and impaired maturation in response to interferon-beta. J Neuropathol Exp Neurol. 2008; 67:388–401. [PubMed: 18431257]

14. Vermi W, Riboldi E, Wittamer V, Gentili F, Luini W, Marrelli S, Vecchi A, Franssen JD, Communi D, Massardi L, Sironi M, Mantovani A, Parmentier M, Facchetti F, Sozzani S. Role of ChemR23 in directing the migration of myeloid and plasmacytoid dendritic cells to lymphoid organs and inflamed skin. J Exp Med. 2005; 201:509–515. [PubMed: 15728234]
15. Kaur J, Adya R, Tan BK, Chen J, Randeva HS. Identification of chemerin receptor (ChemR23) in human endothelial cells: chemerin-induced endothelial angiogenesis. Biochem Biophys Res Commun. 2010; 391:1762–1768. [PubMed: 20044979]
16. Graham KL, Zabel BA, Loghavi S, Zuniga LA, Ho PP, Sobel RA, Butcher EC. Chemokine-like receptor-1 expression by central nervous system-infiltrating leukocytes and involvement in a model of autoimmune demyelinating disease. J Immunol. 2009; 183:6717–6723. [PubMed: 19864606]
17. Huss RS, Huddleston JI, Goodman SB, Butcher EC, Zabel BA. Synovial tissue-infiltrating natural killer cells in osteoarthritis and periprosthetic inflammation. Arthritis Rheum. 2010; 62:3799–3805. [PubMed: 20848566]
18. Weksler BB, Subileau EA, Perriere N, Charneau P, Holloway K, Leveque M, Tricoire-Leignel H, Nicotra A, Bourdoulous S, Turowski P, Male DK, Roux F, Greenwood J, Romero IA, Couraud PO. Blood-brain barrier-specific properties of a human adult brain endothelial cell line. FASEB J. 2005; 19:1872–1874. [PubMed: 16141364]
19. Livak KJ, Schmittgen TD. Analysis of relative gene expression data using real-time quantitative PCR and the 2(−Delta Delta C(T)) Method. Methods. 2001; 25:402–408. [PubMed: 11846609]
20. Sikorski EE, Hallmann R, Berg EL, Butcher EC. The Peyer's patch high endothelial receptor for lymphocytes, the mucosal vascular addressin, is induced on a murine endothelial cell line by tumor necrosis factor-alpha and IL-1. J Immunol. 1993; 151:5239–5250. [PubMed: 7693807]
21. Dauphinee SM, Karsan A. Lipopolysaccharide signaling in endothelial cells. Lab Invest. 2006; 86:9–22. [PubMed: 16357866]
22. Gough DJ, Levy DE, Johnstone RW, Clarke CJ. IFNgamma signaling- does it mean JAK-STAT? *Cytokine Growth Factor Rev* 19:383–394. 2008
23. Peng J, He F, Zhang C, Deng X, Yin F. Protein kinase C-alpha signals P115RhoGEF phosphorylation and RhoA activation in TNF-alpha-induced mouse brain microvascular endothelial cell barrier dysfunction. J Neuroinflammation. 2011; 8:28. [PubMed: 21473788]
24. Kamochi M, Kamochi F, Kim YB, Sawh S, Sanders JM, Sarembock I, Green S, Young JS, Ley K, Fu SM, Rose CE Jr. P-selectin and ICAM-1 mediate endotoxin-induced neutrophil recruitment and injury to the lung and liver. Am J Physiol. 1999; 277:L310–319. [PubMed: 10444525]
25. Youngner JS, Stinebring WR. Interferon appearance stimulated by endotoxin, bacteria, or viruses in mice pre-treated with Escherichia coli endotoxin or infected with Mycobacterium tuberculosis. Nature. 1965; 208:456–458. [PubMed: 4956238]
26. Bertok S, Wilson MR, Dorr AD, Dokpesi JO, O'Dea KP, Marczin N, Takata M. Characterization of TNF receptor subtype expression and signaling on pulmonary endothelial cells in mice. Am J Physiol Lung Cell Mol Physiol. 2011; 300:L781–789. [PubMed: 21378027]
27. Henninger DD, Panes J, Eppihimer M, Russell J, Gerritsen M, Anderson DC, Granger DN. Cytokine-induced VCAM-1 and ICAM-1 expression in different organs of the mouse. J Immunol. 1997; 158:1825–1832. [PubMed: 9029122]
28. Mori N, Horie Y, Gerritsen ME, Anderson DC, Granger DN. Anti-inflammatory drugs and endothelial cell adhesion molecule expression in murine vascular beds. Gut. 1999; 44:186–195. [PubMed: 9895377]
29. Wu X, Guo R, Wang Y, Cunningham PN. The role of ICAM-1 in endotoxin-induced acute renal failure. Am J Physiol Renal Physiol. 2007; 293:F1262–1271. [PubMed: 17670897]
30. Luangsay S, Wittamer V, Bondue B, De Henau O, Rouger L, Brait M, Franssen JD, de Nadai P, Huaux F, Parmentier M. Mouse ChemR23 is expressed in dendritic cell subsets and macrophages, and mediates an anti-inflammatory activity of chemerin in a lung disease model. J Immunol. 2009; 183:6489–6499. [PubMed: 19841182]
31. Hart R, Greaves DR. Chemerin contributes to inflammation by promoting macrophage adhesion to VCAM-1 and fibronectin through clustering of VLA-4 and VLA-5. J Immunol. 2010; 185:3728–3739. [PubMed: 20720202]

32. Lenter M, Uhlig H, Hamann A, Jeno P, Imhof B, Vestweber D. A monoclonal antibody against an activation epitope on mouse integrin chain beta 1 blocks adhesion of lymphocytes to the endothelial integrin alpha 6 beta 1. Proc Natl Acad Sci U S A. 1993; 90:9051–9055. [PubMed: 7692444]

33. Boggemeyer E, Stehle T, Schaible UE, Hahne M, Vestweber D, Simon MM. Borrelia burgdorferi upregulates the adhesion molecules E-selectin, P-selectin, ICAM-1 and VCAM-1 on mouse endothelioma cells in vitro. Cell Adhes Commun. 1994; 2:145–157. [PubMed: 7521760]

34. Erdmann J, Vitale G, van Koetsveld PM, Croze E, Sprij-Mooij DM, Hofland LJ, van Eijck CH. Effects of interferons alpha/beta on the proliferation of human micro- and macrovascular endothelial cells. J Interferon Cytokine Res. 2011; 31:451–458. [PubMed: 21361792]

35. Nagyoszi P, Wilhelm I, Farkas AE, Fazakas C, Dung NT, Hasko J, Krizbai IA. Expression and regulation of toll-like receptors in cerebral endothelial cells. Neurochem Int. 2010; 57:556–564. [PubMed: 20637248]

36. Sikorski K, Chmielewski S, Przybyl L, Heemann U, Wesoly J, Baumann M, Bluyssen HA. STAT1-mediated signal integration between IFNgamma and LPS leads to increased EC and SMC activation and monocyte adhesion. Am J Physiol Cell Physiol. 2011; 300:C1337–1344. [PubMed: 21346151]

37. Yang SK, Wang YC, Chao CC, Chuang YJ, Lan CY, Chen BS. Dynamic cross-talk analysis among TNF-R, TLR-4 and IL-1R signalings in TNFalpha-induced inflammatory responses. BMC Med Genomics. 2010; 3:19. [PubMed: 20497537]

38. Galligan CL, Matsuyama W, Matsukawa A, Mizuta H, Hodge DR, Howard OM, Yoshimura T. Up-regulated expression and activation of the orphan chemokine receptor, CCRL2, in rheumatoid arthritis. Arthritis Rheum. 2004; 50:1806–1814. [PubMed: 15188357]

39. Uhrig A, Banafsche R, Kremer M, Hegenbarth S, Hamann A, Neurath M, Gerken G, Limmer A, Knolle PA. Development and functional consequences of LPS tolerance in sinusoidal endothelial cells of the liver. J Leukoc Biol. 2005; 77:626–633. [PubMed: 15860798]

40. Engelhardt B, Conley FK, Butcher EC. Cell adhesion molecules on vessels during inflammation in the mouse central nervous system. J Neuroimmunol. 1994; 51:199–208. [PubMed: 7514186]

41. Berlin C, Bargatze RF, Campbell JJ, von Andrian UH, Szabo MC, Hasslen SR, Nelson RD, Berg EL, Erlandsen SL, Butcher EC. alpha 4 integrins mediate lymphocyte attachment and rolling under physiologic flow. Cell. 1995; 80:413–422. [PubMed: 7532110]

42. Bozaoglu K, Curran JE, Stocker CJ, Zaibi MS, Segal D, Konstantopoulos N, Morrison S, Carless M, Dyer TD, Cole SA, Goring HH, Moses EK, Walder K, Cawthorne MA, Blangero J, Jowett JB. Chemerin, a novel adipokine in the regulation of angiogenesis. J Clin Endocrinol Metab. 2010; 95:2476–2485. [PubMed: 20237162]

43. Fan P, Kyaw H, Su K, Zeng Z, Augustus M, Carter KC, Li Y. Cloning and characterization of a novel human chemokine receptor. Biochem Biophys Res Commun. 1998; 243:264–268. [PubMed: 9473515]

44. Mantovani A, Bonecchi R, Locati M. Tuning inflammation and immunity by chemokine sequestration: decoys and more. Nat Rev Immunol. 2006; 6:907–918. [PubMed: 17124512]

45. Naumann U, Cameroni E, Pruenster M, Mahabaleshwar H, Raz E, Zerwes HG, Rot A, Thelen M. CXCR7 functions as a scavenger for CXCL12 and CXCL11. PLoS One. 2010; 5:e9175. [PubMed: 20161793]

46. Dawson TC, Lentsch AB, Wang Z, Cowhig JE, Rot A, Maeda N, Peiper SC. Exaggerated response to endotoxin in mice lacking the Duffy antigen/receptor for chemokines (DARC). Blood. 2000; 96:1681–1684. [PubMed: 10961863]

47. Jamieson T, Cook DN, Nibbs RJ, Rot A, Nixon C, McLean P, Alcami A, Lira SA, Wiekowski M, Graham GJ. The chemokine receptor D6 limits the inflammatory response in vivo. Nat Immunol. 2005; 6:403–411. [PubMed: 15750596]

48. Rot A. Contribution of Duffy antigen to chemokine function. Cytokine Growth Factor Rev. 2005; 16:687–694. [PubMed: 16054417]

49. Nibbs RJ, Kriehuber E, Ponath PD, Parent D, Qin S, Campbell JD, Henderson A, Kerjaschki D, Maurer D, Graham GJ, Rot A. The beta-chemokine receptor D6 is expressed by lymphatic

endothelium and a subset of vascular tumors. Am J Pathol. 2001; 158:867–877. [PubMed: 11238036]

50. Miao Z, Luker KE, Summers BC, Berahovich R, Bhojani MS, Rehemtulla A, Kleer CG, Essner JJ, Nasevicius A, Luker GD, Howard MC, Schall TJ. CXCR7 (RDC1) promotes breast and lung tumor growth in vivo and is expressed on tumor-associated vasculature. Proc Natl Acad Sci U S A. 2007; 104:15735–15740. [PubMed: 17898181]
51. Bondue B, Vosters O, de Nadai P, Glineur S, De Henau O, Luangsay S, Van Gool F, Communi D, De Vuyst P, Desmecht D, Parmentier M. ChemR23 dampens lung inflammation and enhances anti-viral immunity in a mouse model of acute viral pneumonia. PLoS Pathog. 2011; 7:e1002358. [PubMed: 22072972]
52. Maus UA, Wellmann S, Hampl C, Kuziel WA, Srivastava M, Mack M, Everhart MB, Blackwell TS, Christman JW, Schlondorff D, Bohle RM, Seeger W, Lohmeyer J. CCR2-positive monocytes recruited to inflamed lungs downregulate local CCL2 chemokine levels. Am J Physiol Lung Cell Mol Physiol. 2005; 288:L350–358. [PubMed: 15516494]
53. Zabel BA, Zuniga L, Ohyama T, Allen SJ, Cichy J, Handel TM, Butcher EC. Chemoattractants, extracellular proteases, and the integrated host defense response. Exp Hematol. 2006; 34:1021–1032. [PubMed: 16863908]
54. Esmon CT, Esmon NL. The link between vascular features andthrombosis. Annu Rev Physiol. 2011; 73:503–514. [PubMed: 20887194]
55. Van de Wouwer M, Collen D, Conway EM. Thrombomodulin-protein C-EPCR system: integrated to regulate coagulation and inflammation. Arterioscler Thromb Vasc Biol. 2004; 24:1374–1383. [PubMed: 15178554]
56. Demoor T, Bracke KR, Dupont LL, Plantinga M, Bondue B, Roy MO, Lannoy V, Lambrecht BN, Brusselle GG, Joos GF. The role of ChemR23 in the induction and resolution of cigarette smoke-induced inflammation. J Immunol. 2011; 186:5457–5467. [PubMed: 21430224]
57. Otero K, Vecchi A, Hirsch E, Kearley J, Vermi W, Del Prete A, Gonzalvo-Feo S, Garlanda C, Azzolino O, Salogni L, Lloyd CM, Facchetti F, Mantovani A, Sozzani S. Nonredundant role of CCRL2 in lung dendritic cell trafficking. Blood. 2010; 116:2942–2949. [PubMed: 20606167]
58. Lau EK, Allen S, Hsu AR, Handel TM. Chemokine-receptor interactions: GPCRs, glycosaminoglycans and viral chemokine binding proteins. Adv Protein Chem. 2004; 68:351–391. [PubMed: 15500866]
59. Catusse J, Leick M, Groch M, Clark DJ, Buchner MV, Zirlik K, Burger M. Role of the atypical chemoattractant receptor CRAM in regulating CCL19 induced CCR7 responses in B-cell chronic lymphocytic leukemia. Mol Cancer. 2010; 9:297. [PubMed: 21092185]

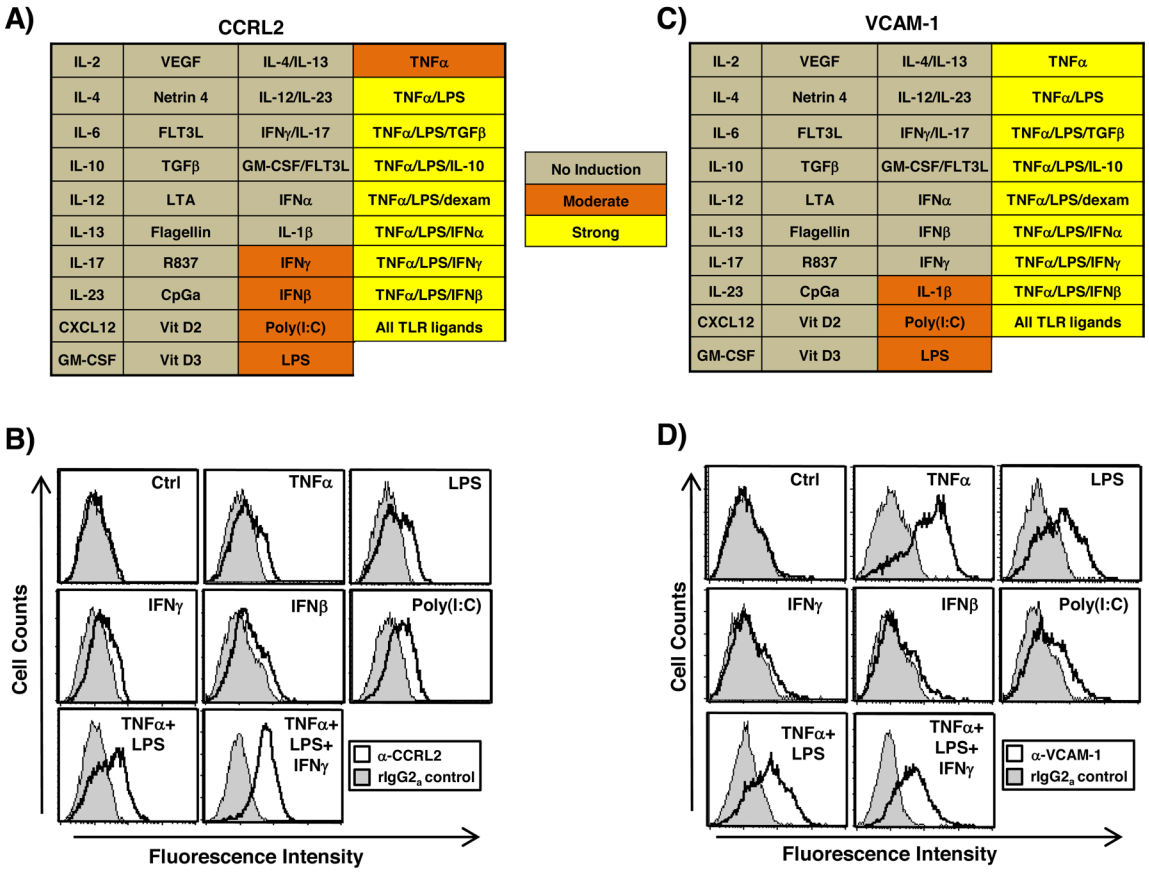

Figure 1. Selective upregulation of CCRL2 and VCAM-1 in endothelioma cells by proinflammatory stimuli

CCRL2 **(A)** and VCAM-1 **(B)** protein expression were measured by flow cytometry on mouse brain endothelioma cells (bEND.3) treated for 24h with the indicated soluble inflammatory mediator(s). The induction of CCRL2 and VCAM-1 is represented as a heat map. Histogram plots of CCRL2 (**C**) and VCAM-1 (**D**) are representative of the induction of CCRL2 and VCAM-1. Representative of n=3 independent experiments.

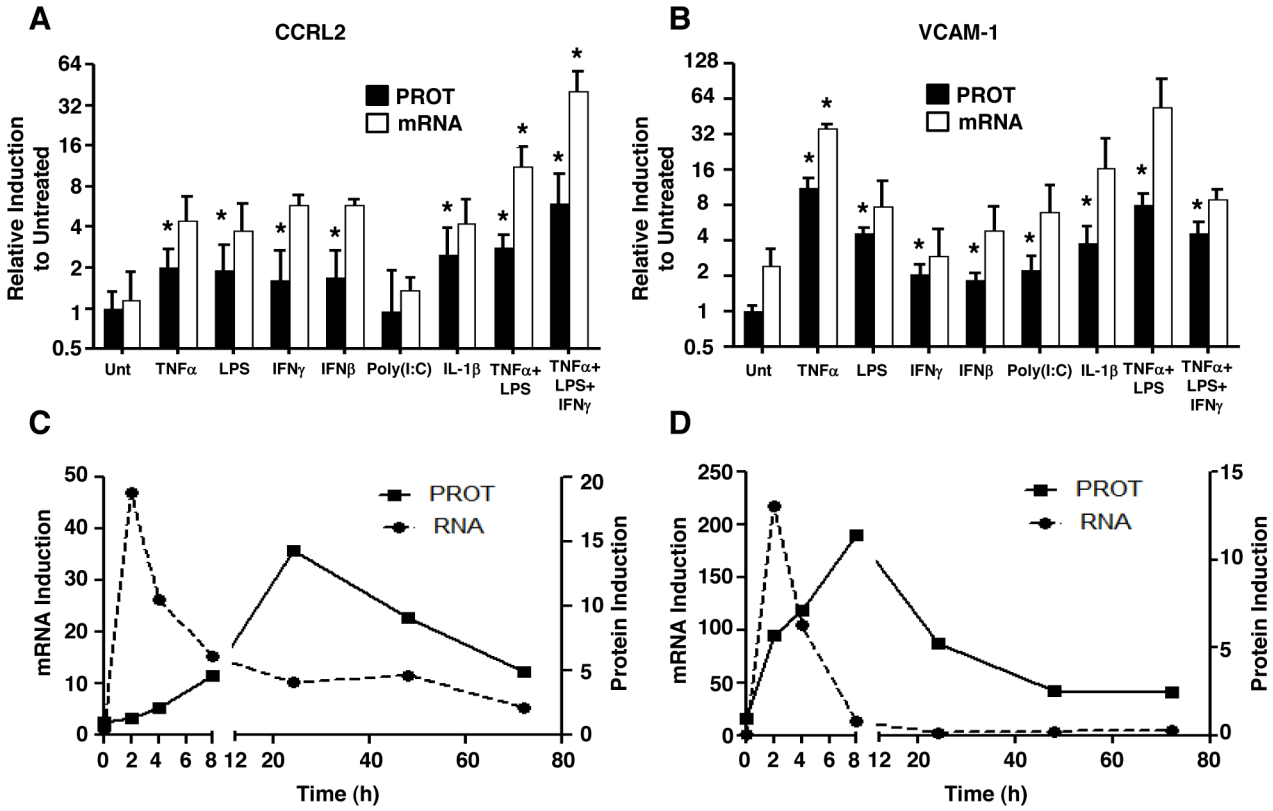

Figure 2. Kinetic analysis of CCRL2 and VCAM-1 induction

CCRL2 (**A**) and VCAM-1 (**B**) mRNA and protein induction was measured in bEND.3 cells treated with the indicated cytokines for 24h. The mean of n=3 different experiments ± SD is shown. *p<0.05 by *t*-test. TNFα+ LPS+ IFNγ were incubated with bEND.3 cells for the indicated times. At each time point CCRL2 (**C**) and VCAM-1 (**D**) induction was measured by either RT-QPCR (normalized to CDC42), or by mAb staining and flow cytometry. Data points represent the mean of 2–3 experiments.

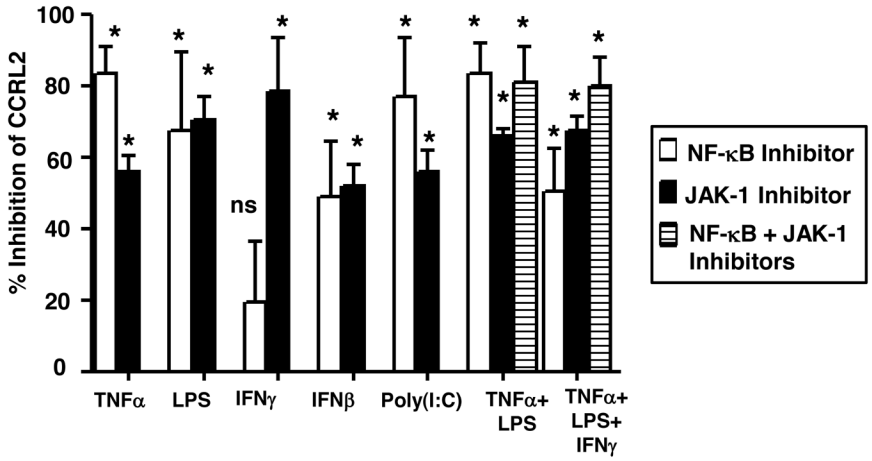

Figure 3. NF-κB and JAK/STAT signaling pathways regulate CCRL2 induction in endothelial cells

Mouse bEND.3 cells were pre-incubated with IKKβ inhibitor BAY (11–7082) and/or with JAK-1 inhibitor (sc-204021) followed by incubation with the indicated cytokines and TLR ligands. CCRL2 protein expression was measured by flow cytometry. Blocking of CCRL2 induction by specific inhibitors is displayed as a percent inhibition. The mean of n=5–8 different experiments ± SD is shown. *p<0.05 by *t*-test.

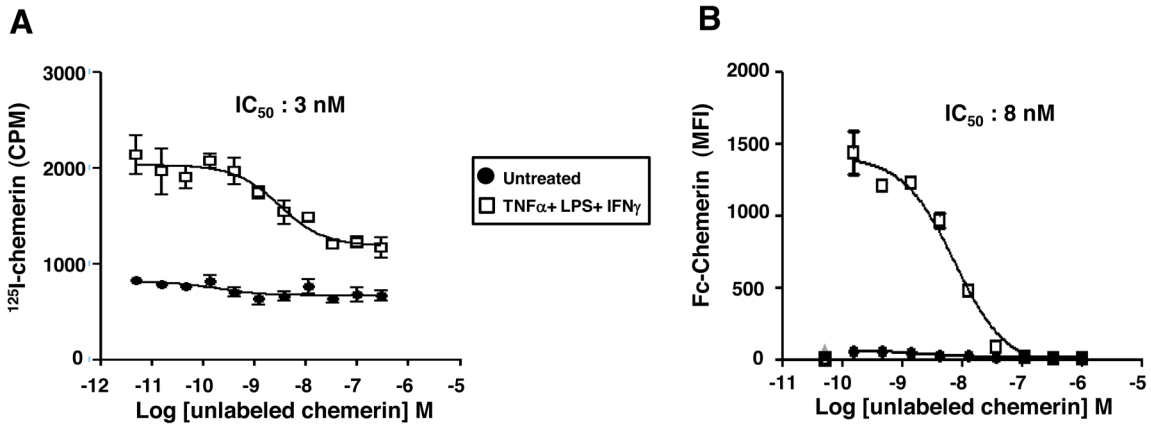

Figure 4. Chemerin binds to activated bEND.3 cells

bEND.3 cells were activated with TNF-α plus LPS plus IFN-γ for 24 h and incubated with either [^{125}I]chemerin (**A**) or Fc-Chemerin (**B**) in the presence of various concentrations of unlabeled chemerin competitor. The mean of triplicate wells ± SD is shown for each experiment. Data shown are representative of three individual experiments with similar results.

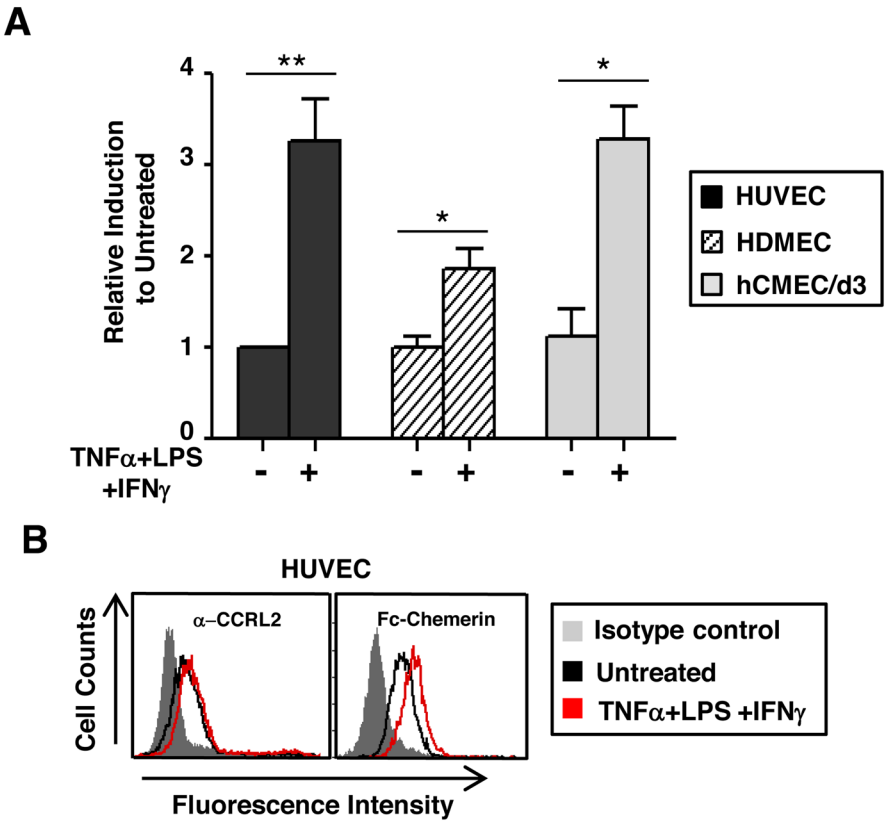

Figure 5. Human endothelial cells upregulate CCRL2

Human umbilical vein endothelial cells (HUVEC), human dermal microvascular cells (HDMEC) and a human brain endothelial cell line (hCMEC/d3) were incubated for 24 h with TNF-α plus LPS plus IFN-γ. (**A**) Induction of CCRL2 RNA was measured in all samples by RT-qPCR normalized to β-actin. The means of three different experiments ± SD are shown. *p<0.05, **p<0.01 by t-test. (**B**) HUVECs were either untreated or treated with TNF-α plus LPS plus IFN-γ for 24 h and stained for CCRL2 expression and Fc-chemerin binding. Results are representative of three individual experiments with similar results.

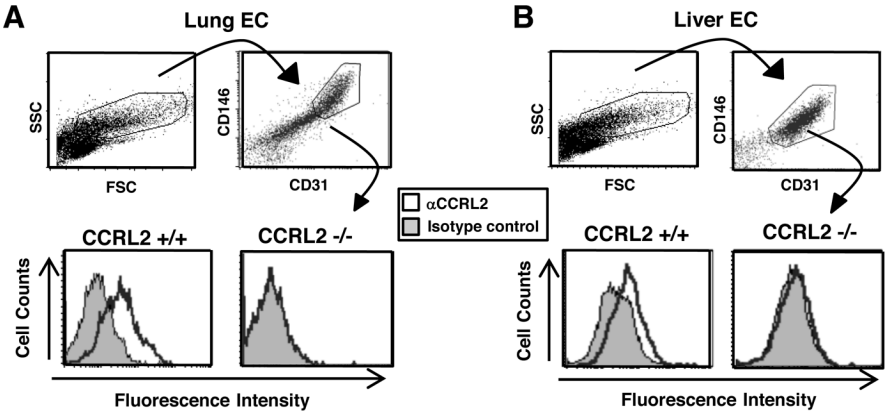

Figure 6. CCRL2 protein expression in mouse primary EC

After collagenase digestion and endothelial enrichment by density gradient, lung (**A**) and liver (**B**) EC from WT and CCRL2−/− mice were evaluated for CCRL2 expression. CD31 and CD146 were used to identify EC by flow cytometry. Data shown are representative of three different experiments with similar results.

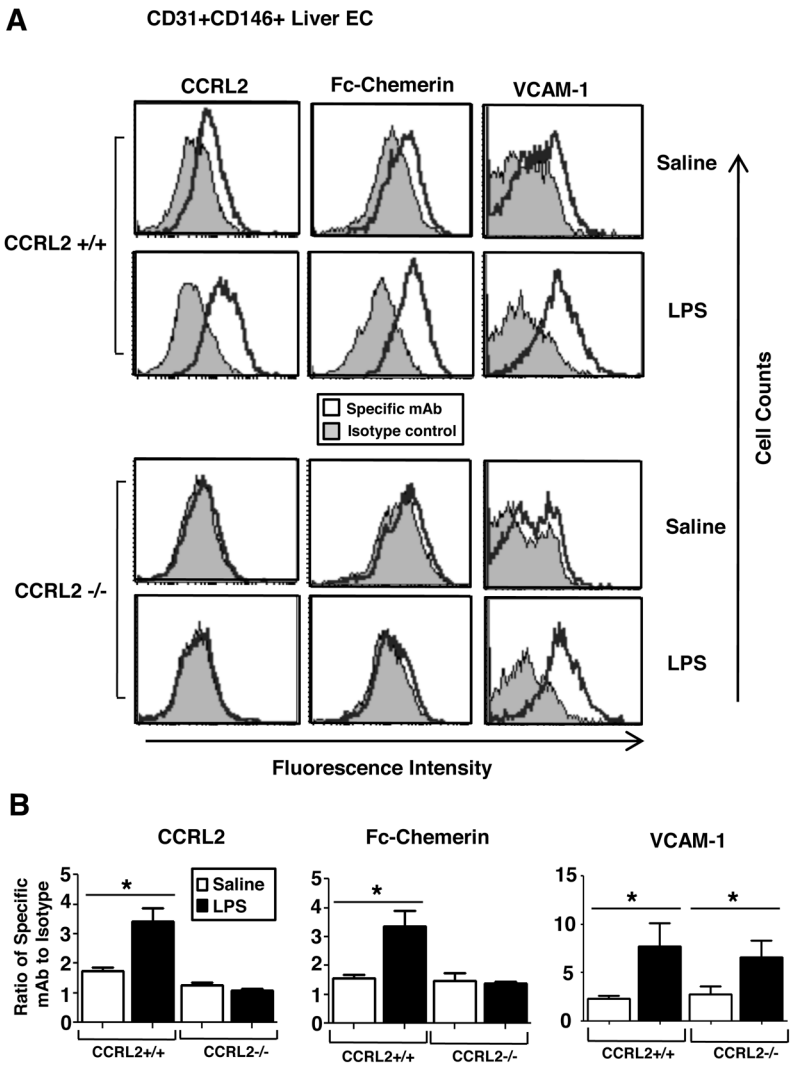

Figure 7. CCRL2 upregulation on mouse liver endothelial cells following LPS injection *in vivo*

Wild-type or CCRL2−/− mice were injected i.p. with LPS. Endothelial cells from the liver were isolated 12 hours later, enriched and identified by co-staining for CD31 and CD146. Surface expression of CCRL2 on these cells was determined using anti-mCCRL2 and Fc-Chemerin (**A**). VCAM-1 expression was determined by flow cytometry (**B**). The data set shown is representative of 3–6 individual experiments with similar results. (**C**) Induction of CCRL2, Fc-Chemerin and VCAM-1 in LPS treated mice was quantified by normalizing the specific antibody MFI value to its isotype MFI value. The mean ± SEM is shown. Each graph represents 3–6 independent experiments pooled together (n=1–2 mice per group per experiment).*p<0.05 by *t*-test.

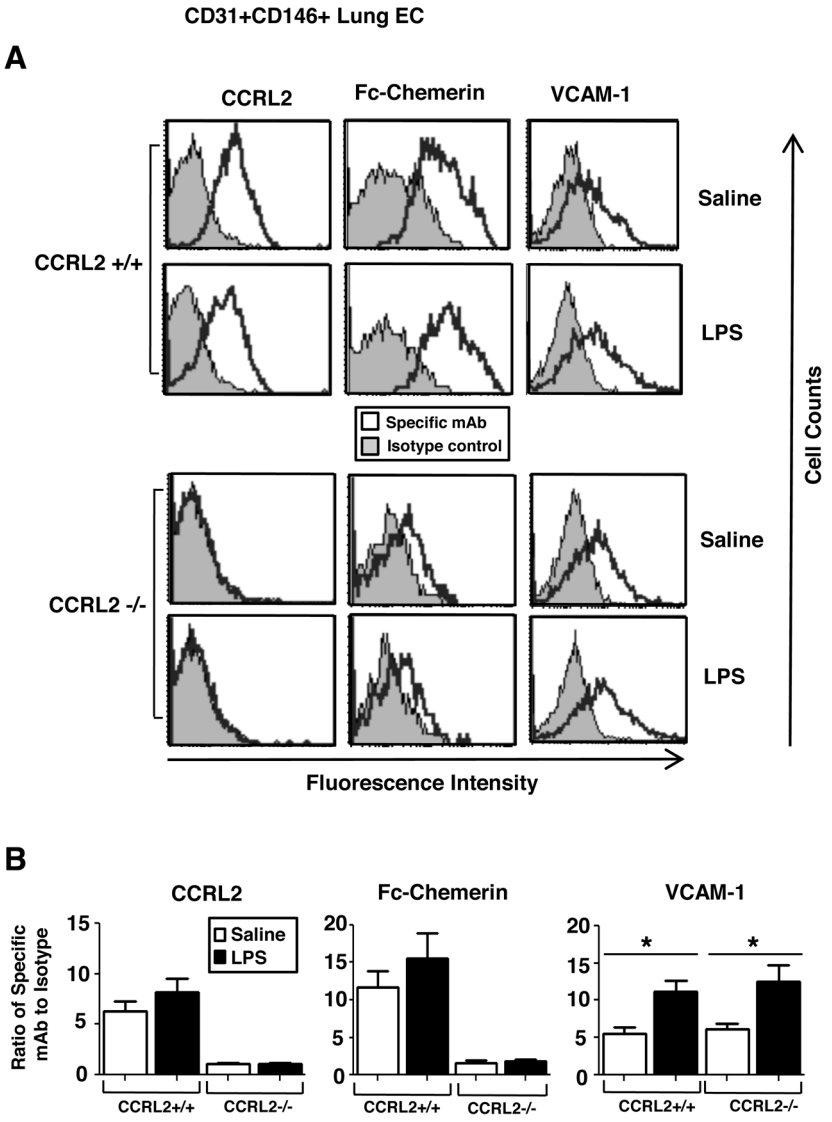

Figure 8. LPS injection does not alter CCRL2 expression on mouse lung endothelial cells *in vivo*

Wild-type or CCRL2 KO mice were injected i.p. with LPS. Endothelial cells from the lung were isolated 12 hours later, enriched and identified by co-staining for CD31 and CD146. Surface expression of CCRL2 on these cells was determined using anti-mCCRL2 and Fc-Chemerin (**A**). VCAM-1 expression was determined by flow cytometry (**B**). The data set shown is representative of 3–6 individual experiments with similar results. (**C**) Induction of CCRL2, Fc-Chemerin and VCAM-1 in LPS treated mice was quantified by normalizing the specific antibody MFI value to its isotype MFI value. The mean ± SEM is shown. Each graph represents 3–6 independent experiments pooled together (n=1–2 mice per group per experiment).*p<0.05 by *t*-test.

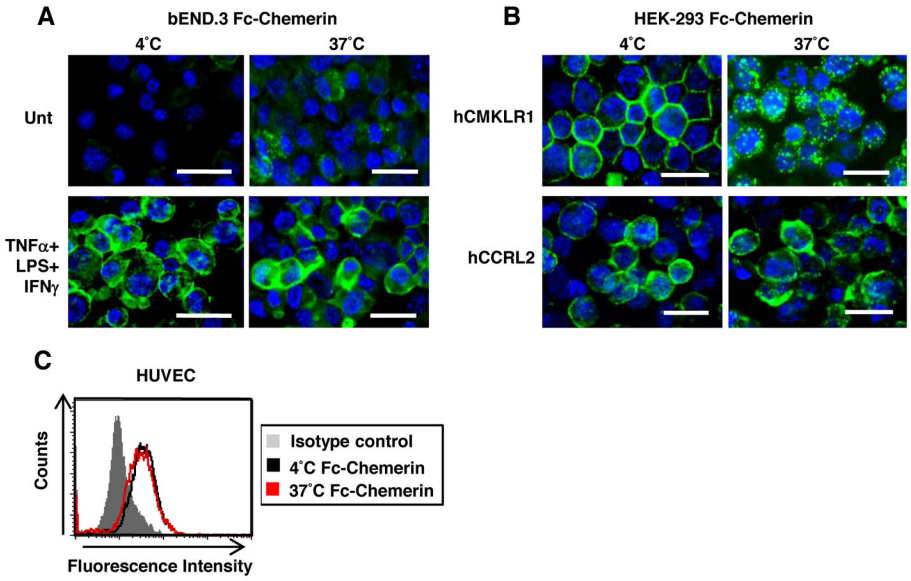

Figure 9. CCRL2+ endothelial cells bind but do not internalize chemerin

HEK-293 cells transfected with hCCRL2 or hCMKLR1 (**A**) as well as bEND.3 cells treated with or without TNFα + LPS + IFNγ (**B**)were pre-incubated with Fc-Chemerin and goat-anti-mouse IgG-Alexa 488 at 4°C, and then shifted to 4oC or 37oC. Internalization of fluorescently labeled Fc-Chemerin was monitored by fluorescent microscopy. The data set shown is representative of 3 individual experiments with similar results. Bar = 25 μm. (**C)** HUVECs pre-treated for 24h with TNFα + LPS + IFNγ were incubated with Fc-Chemerin at 4°C for 30 minutes. Cells were washed to remove unbound chemerin and then shifted to either 4°C or 37°C for 30 minutes. Surface bound Fc-Chemerin was detected using rat-anti-mouse IgG1-PE secondary antibody. Representative of n=3 individual experiments with similar results.

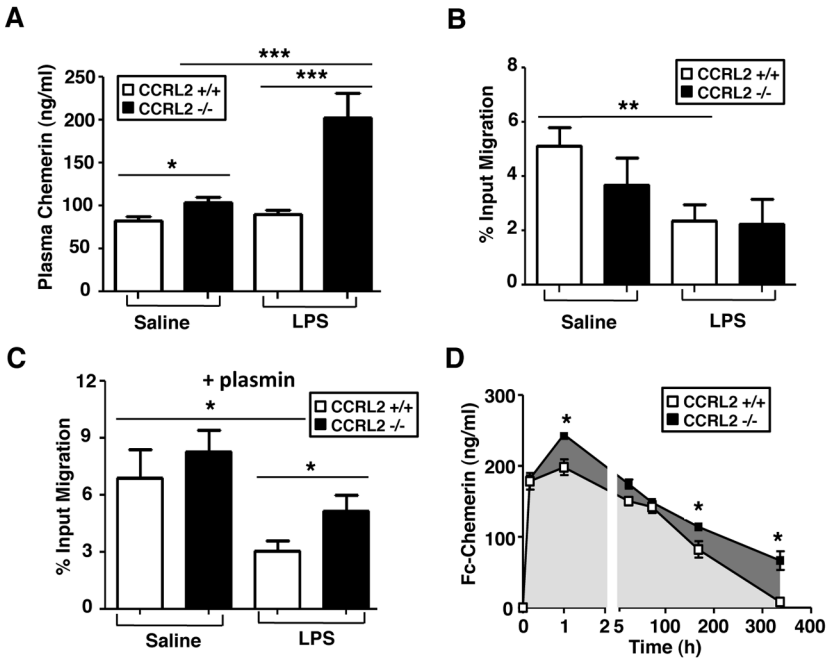

Figure 10. CCRL2 regulates circulating chemerin levels and its bioactivity *in vivo*

(**A**) Wild-type and CCRL2−/− mice were either untreated or injected with 12 mg/kg LPS for 12 hours, after which chemerin levels in plasma was measured by ELISA. For untreated mice, the mean of n=100 (WT) and n=92 (CCRL2−/−) individual mice ± SEM is shown. For LPS-treated mice, the mean of n=6 individual mice ± SEM is shown. *p<0.05, ***p<0.001 by *t*-test. (**B**) The chemotactic bioactivity of plasma chemerin from WT and CCRL2−/− mice ± LPS treatment was evaluated by *in vitro* mCMKLR1/L1.2 cell migration. **p<0.01 by *t*-test. (**C**) Plasma pro-chemerin levels were evaluated by pre-incubating plasma samples with plasmin to proteolytically activate chemerin and then assessing mCMKLR1/L1.2 cell migration. For (**B**) and (**C**), the mean of n=9–10 mice ± SD is shown. *p<0.05 by *t*-test. Representative of n=2 independent experiments. (**D**) 3 μg of Fc-Chemerin was injected i.v. in WT or CCRL2−/− mice and Fc-Chemerin plasma levels were quantified at the indicated time points. The mean of n=3 mice ± SD is shown. Statistical significance was determined by ANOVA followed by Bonferonni posthoc test. (*p<0.05)

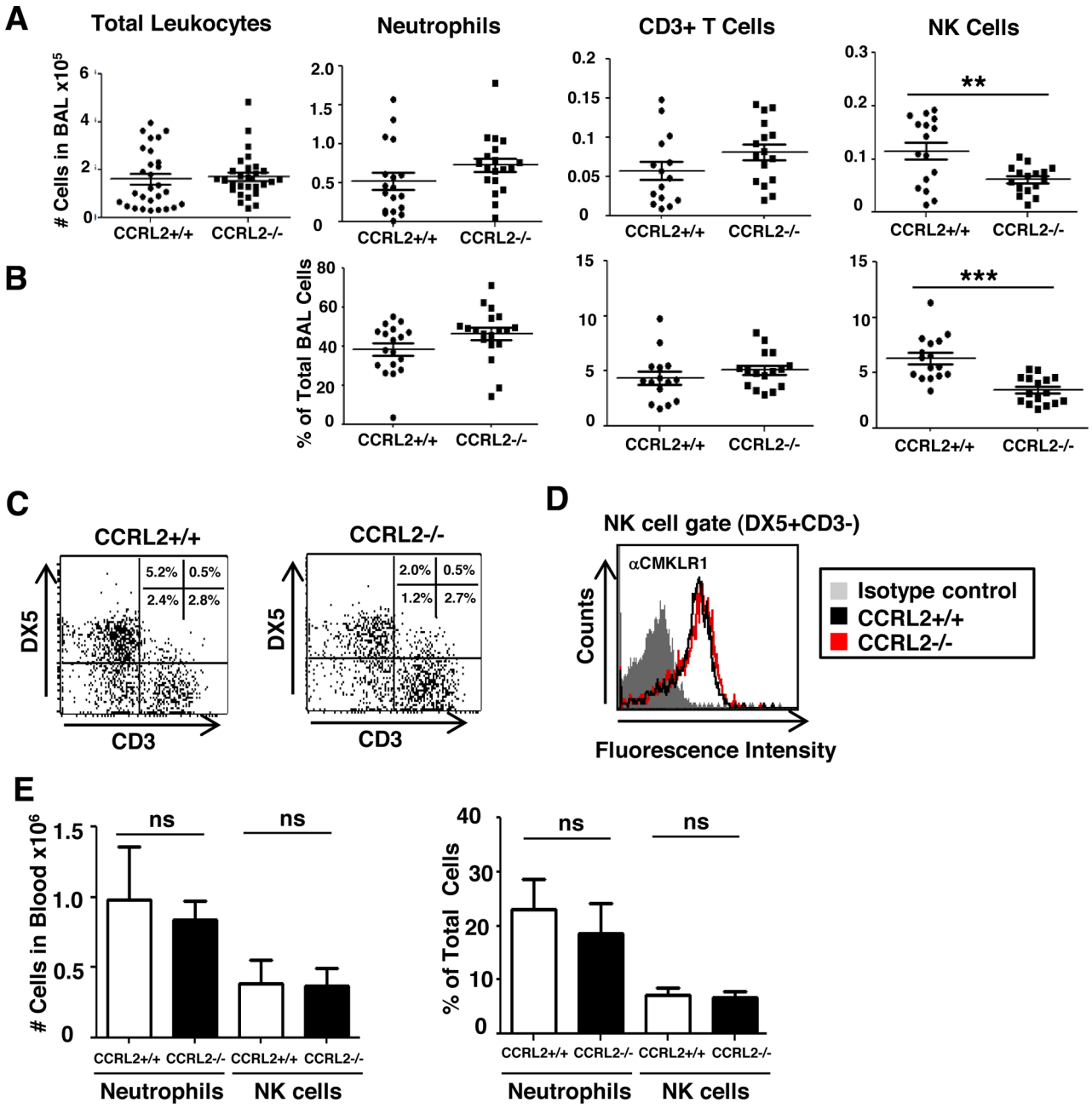

Figure 11. Impaired *in vivo* recruitment of CMKLR1+ NK cells into inflamed airways in CCRL2−/− mice

Following intranasal LPS administration, BAL fluid from WT and CCRL2−/− mice was collected and cells stained for neutrophils (Ly6G), T cells (CD3) and NK-cells (DX5), and plotted either as absolute number of infiltrating cells (**A**) or as a percentage of total BAL leukocytes (**B**). Each graph represents 3–4 independent experiments pooled together (n=15–29 mice per group; each symbol represents one mouse). **p<0.01, ***p<0.001 by *t*-test. (**C**) Representative flow cytometry dot plots of CD3 vs. DX5 staining of BAL cells from WT and CCRL2 −/− mice. (**D**) Blood NK cells (DX5+CD3-) from WT or CCRL2−/− mice were stained for CMKLR1. Representative histogram of n=3 independent experiments. White blood cells were collected from WT and CCRL2−/− mice, stained for neutrophils (Ly6G)

and NK cells (CD3-DX5+), and plotted either as absolute number (**E**) or as a percentage of total leukocytes. n=3 mice per group.

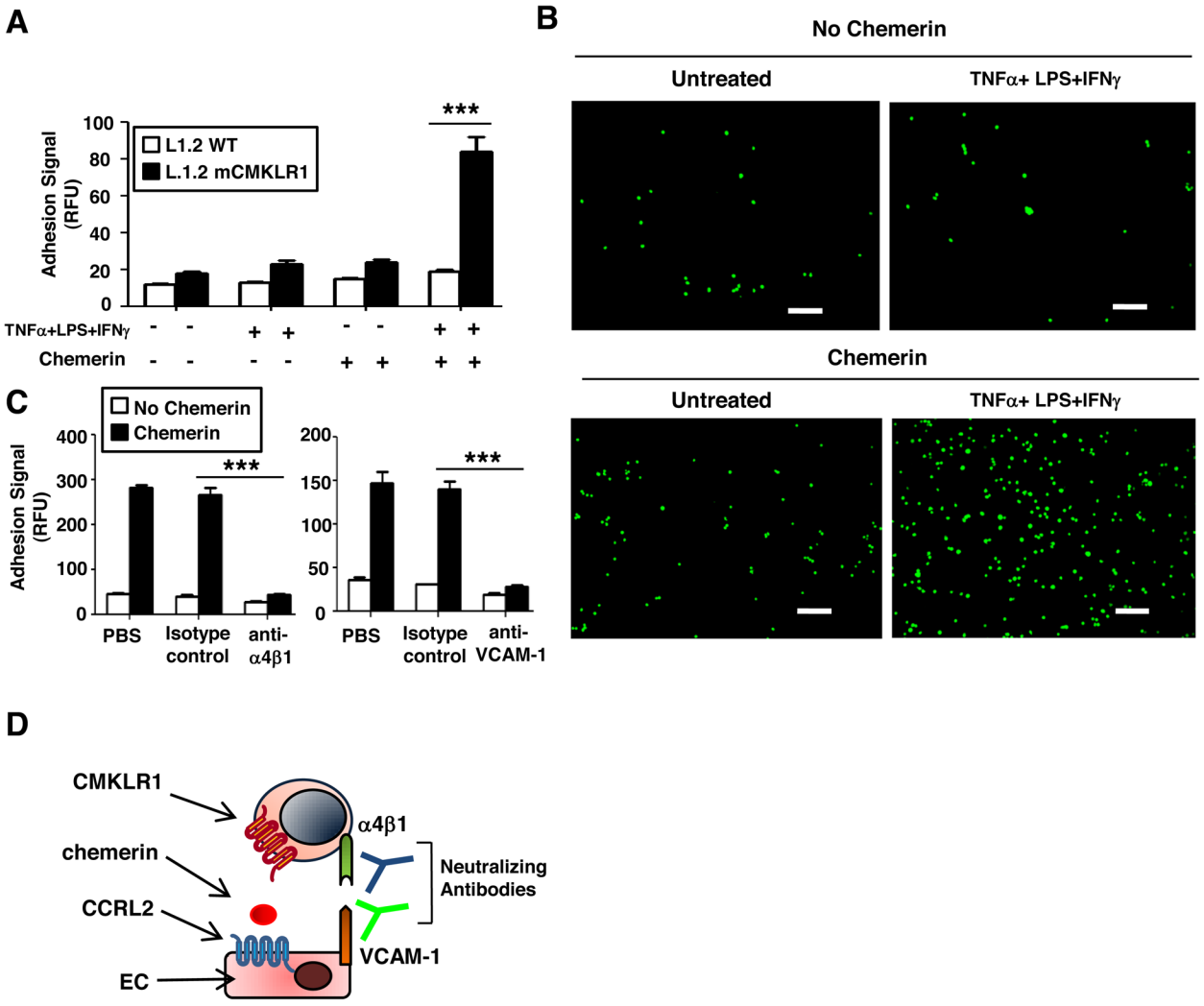

Figure 12. CCRL2+ activated endothelial cells bind chemerin and trigger CMKLR1+ cell adhesion

(**A**) Mouse bEND.3 cells were untreated or treated with TNFα ± LPS + IFNγ, loaded with chemerin, and then co-incubated with WT or CMKLR1+ L1.2 lymphoid cells pre-labeled with calcein AM. The mean of quintuplet wells ± SD of n=3 independent experiments with similar results is shown. (**B**) Fluorescent microscopy of adherent CMKLR1+ cells. Panels show adhesion of L1.2-CMKLR1+ cells to bEND.3 cells treated ± TNFα ± LPS + IFNγ and ± chemerin. Representative images of n=3 different experiments. Bar = 25 μm. (**C**) Left panel: Inhibition of L.12-CMKLR1+ cell adhesion to bEND.3 cells was evaluated by pre-incubating L1.2-CMKLR1+ cells either with PBS, rat IgG isotype control or with rat-anti-mouse α4. Right Panel: Inhibition of L.12-CMKLR1+ cell adhesion to bEND.3 cells was evaluated by pre-incubating bEND.3 cells with either PBS, rat IgG isotype control or with rat-anti-mouse VCAM-1. The mean of quintuplet wells ± SD of n=3 independent experiments with similar results is shown. ***p<0.001 by *t*-test. (**D**) Model summarizing the components involved in chemerin-dependent CMKLR1+ cell adhesion to CCRL2+ EC.